Mater. Res. Soc. Symp. Proc. Vol. 1432 © 2012 Materials Research Society
DOI: 10.1557/opl.2012.1055

Reduction of Triangular Defects on 100mm 4° off-axis 4H-SiC using a Chloride Based CVD process

Hrishikesh Das [a], Swapna Sunkari, Timothy Oldham, Josh Rodgers, and Janna Casady

SemiSouth Laboratories, Inc. 201 Research Blvd., Starkville, MS, 39759, USA

[a]hrishikesh.das@semisouth.com,

Keywords: 6 x 4 inch planetary reactor, epitaxial growth, 4º off-axis, triangular defects, chloride CVD process

ABSTRACT

Homoepitaxial layers were grown with very low surface roughness on 4", 4˚ off-axis substrates, but a new kind of large obtuse angled triangular defect that spanned 1000-2000 μm was observed. Process changes resulted in reduction of the size and concentration of these triangular defects from 3.5cm^{-2} to 0.13cm^{-2}. Both large and small triangular defects were found to have a similar core structure. No degradation in the epitaxial morphology or quality was seen due to the process change. JBS diodes fabricated on wafers with large triangular defects had much higher leakage when the triangular defects were present in the active area of the diodes.

INTRODUCTION

Silicon carbide is a material of choice for fabricating low-loss power devices. Significant advances in the growth of homo-epitaxial layers on good quality substrates have led to the availability of high performance commercial SiC power devices. Zero micropipe density (MPD) substrates are commercially available, and good quality epitaxial layers grown on these substrates that are free from morphological defects like triangles, pits and comets can drastically boost the performance of these SiC power devices. Triangular defects are a commonly occurring defect on lower off-cut angle (4º off-axis or lower) substrates, due to larger terrace widths that promote 2D nucleation. This increases the chances for triangular defect formation [1,2]. Other factors can also cause formation of the triangular defects like substrate defects [3], high C/Si ratios [4] or lower temperatures [5]. Triangular defects also have a tendency to form when there is an interruption in the step flow growth caused by particles, Si droplets or nucleating islands [5]. Triangular defects that have been studied do not have very wide angles [6]. Recently Chung et al. reported observing much wider triangular defects with obtuse angles [7].

In our previous work, we reported process enhancements that resulted in very smooth epitaxial layers that are free of step-bunching [8]. However large obtuse angled triangular defects like [7] were observed. In this work we present process changes implemented in our 6x4" reactor that reduces the nucleation of these triangular defects from particles and other factors. The structure of the triangular defects is characterized by molten potassium hydroxide etching. Junction barrier diodes are fabricated to assess the impact of these defects on device leakage performance.

EXPERIMENTAL

The epitaxial growth was conducted in an Aixtron VP2400, a commercial multi-wafer hot-wall CVD planetary reactor. Commercially available 4 inch, n-type, 4˚ off-axis, Si-face 4H-SiC substrates were used for this work. The epitaxial growth was conducted with a H_2 – SiH_4 – C_3H_8 – HCl chemistry. The growth pressure was varied from 100mbar to 200mbar, while the growth temperature was varied between 1600-1650˚C. The C/Si ratio, Cl/Si ratio and H_2 flows were varied to establish the optimal conditions for triangular defect reduction and good morphology.

Nomarski Microscopy, Laser Light Scattering surface scans, Atomic Force Microscopy (AFM), Molten Potassium Hydroxide (KOH) etching and X-Ray Diffraction (XRD) were used to characterize the epitaxial layers. Laser Light scattering surface characterization of the epitaxial layers was done with a KLA Tencor Candela CS10 system. AFM measurements were done on a Dimension Icon AFM system with ScanAsyst on 10µm x 10µm areas. Molten KOH etching was performed in a nickel crucible at a temperature of 600°C for 5 minutes. XRD was acquired with a PANalytical X'Pert MRD 6-axis diffractometer equipped with a Copper X-ray tube and sealed proportional detector.

5A 1200V Junction Barrier Schottky diodes having an area of 2.8mm^2 were fabricated on the characterized wafers to gain statistical leakage data due to the effect of various defects. Leakage currents were measured on over 2300 devices.

RESULTS AND DISCUSSION

Epitaxial layers grown using standard silane, propane and HCl chemistry have been demonstrated to have very low surface roughness of 0.32nm [8]. These layers were grown at a low growth rate (LGR) of 8µm/hr with a low Cl/Si ratio. Very large triangular defects were seen nucleating in these epitaxial layers. Many of the triangular defects nucleated from visible particles at their heads, while a few defects nucleated without any accompanying defects or particles. The size of the triangular defects ranged from 1000µm to 2000µm. Figure 1a shows the Nomarski micrograph of a few triangular defects nucleating at particles of different sizes.

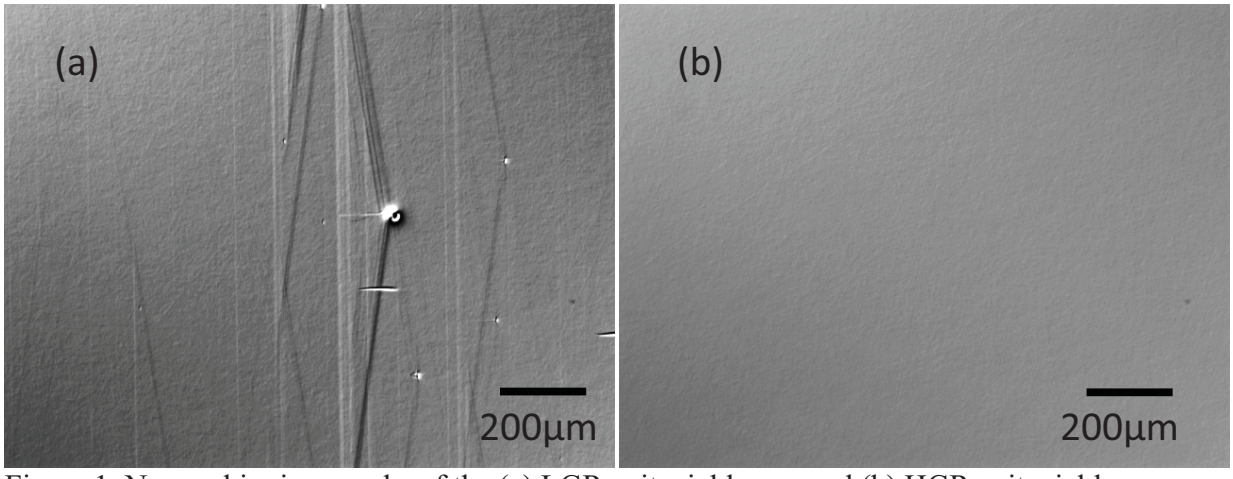

Figure 1. Nomarski micrographs of the (a) LGR epitaxial layers and (b) HGR epitaxial layers

To reduce the formation of these triangular defects, process conditions were changed to reduce the size and nucleation of these large triangles. A much higher growth rate (HGR) of 30µm/hr with a higher Cl/Si ratio was used to obtain almost triangular defect free epitaxial layers. Figure 1b shows the Nomarski micrograph of a HGR epitaxial layer. Very few large triangular defects were seen in the HGR epi. Most of the triangular defects that were detected were much smaller in size.

A special Candela scan recipe was developed that detected only triangular defects to statistically differentiate between the LGR and HGR processes. Particles and other surface defects were excluded from this detection. However if a triangular defect formed around a particle or any other defect, it was included in the detection recipe. Figure 2 shows the full wafer Candela scans of LGR and HGR epitaxial wafers. The density of the large triangular defects reduces drastically from $3.5cm^{-2}$ to $0.13cm^{-2}$.

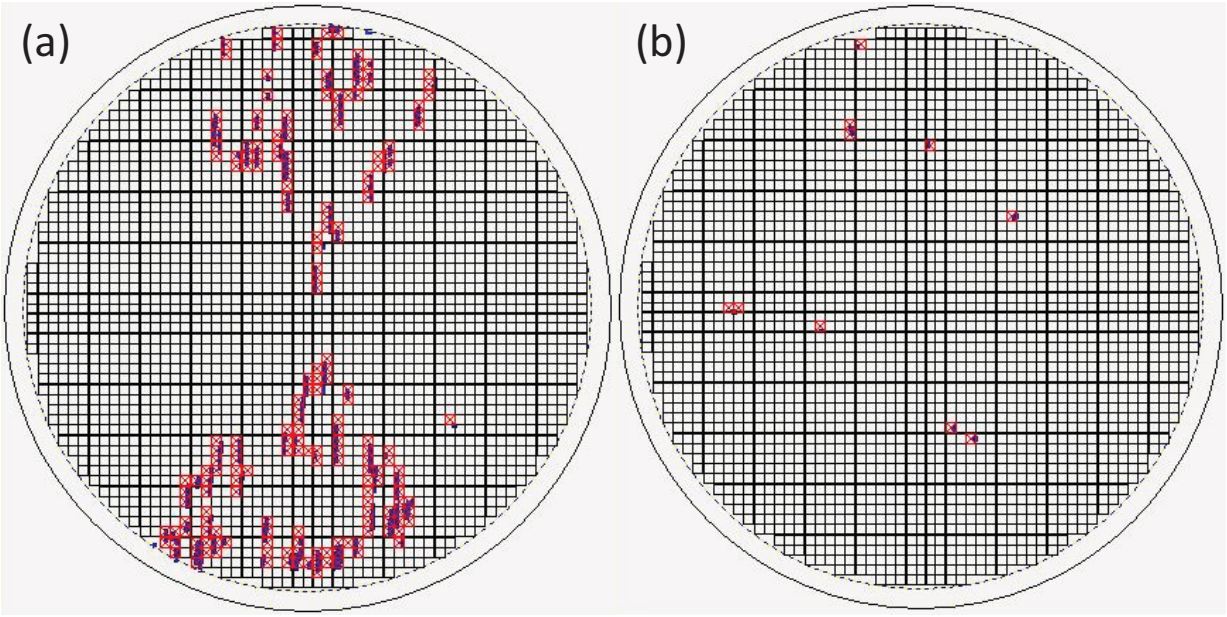

Figure 2. Full wafer Candela scans enumerating the large triangular defects in (a) LGR epi ($3.5cm^{-2}$) and (b) HGR epi ($0.13cm^{-2}$)

Figure 3 shows both the LGR and HGR Candela surface scan images from the regions with the worst triangular defects. Figure 3a shows both the nucleation of triangular defects from visible particles and triangular defects without any attached defects on the LGR epi. Figure 3b shows a much more magnified view of the triangular defects that are nucleated in the HGR epi. These triangular defects are smaller in size ranging from 50µm to 150µm. Figure 3b also shows a particle pit that does not nucleate into a triangular defect. This is a characteristic of the HGR process and is seen all over on the HGR epi wafers. In the LGR epi wafers, such particles almost always invariably nucleate triangular defects.

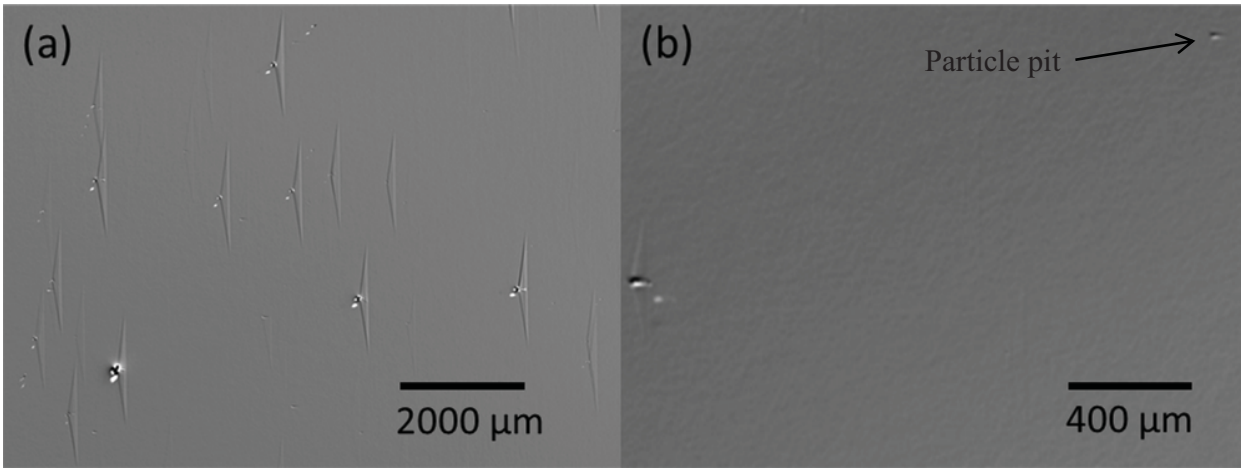

Figure 3. Candela scan images showing triangular defects in (a) LGR epi and (b) HGR epi

Molten KOH etching was done on both LGR and HGR epi wafers to delineate the defects and determine the structure and differences in the triangular defects. An etch of 5 minutes at 600°C was enough to properly delineate all the defects. Figure 4 shows the Nomarski micrographs of molten KOH etch delineated defects in the LGR and HGR epi. Figure 4b shows a triangular defect in the HGR epi which consists of a threading dislocation at the head and bound by basal plane dislocations (BPDs) and a stacking fault (SF). The triangular defect itself is relatively small at less than 100µm as expected from Figure 3b. Figure 4a shows the triangular defect in the LGR epi. The dashed lines show the long wings of the triangular defect spanning more than 1000µms in length. The interesting thing is that even these large triangular defects have a smaller sized core that has a similar size and structure as the triangular defect structures on the HGR epi. The long wings do not show any delineated defects during the span or at the ends.

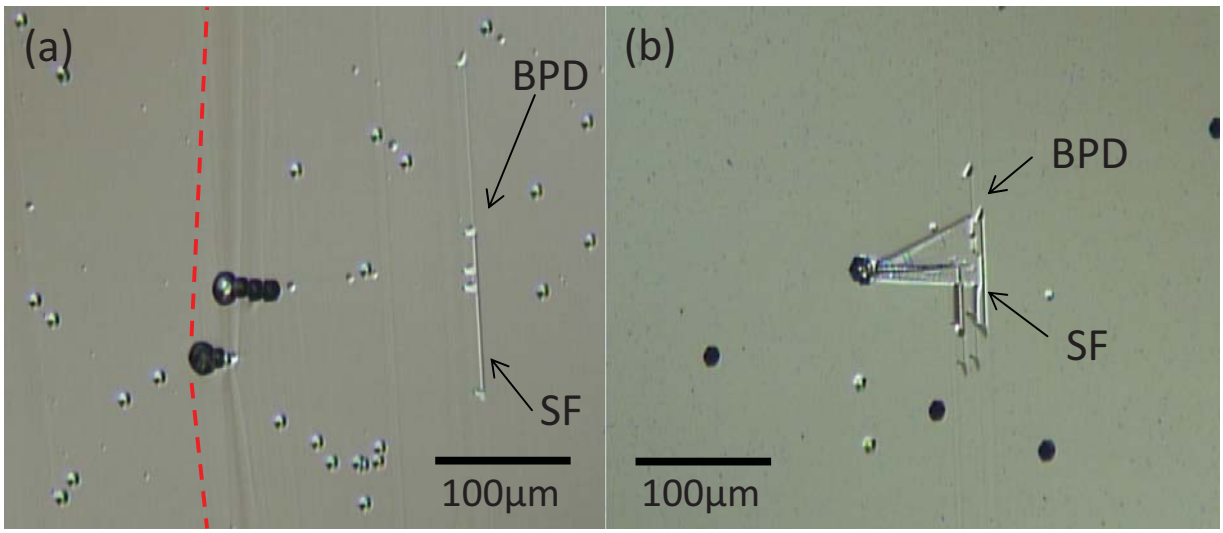

Figure 4. Molten KOH etched image of triangular defects on (a) LGR epi and (b) HGR epi

The effect of the higher growth rate and higher Cl/Si ratio on surface morphology and crystalline quality was evaluated using AFM scans and XRD rocking curves. Figure 5 shows the AFM

scans of both LGR and HGR epi with a thickness of 15µm. The RMS surface roughness is very comparable at 0.32nm and 0.34nm for the LGR and HGR epi respectively. XRD rocking curve measurements were performed for both LGR and HGR epi and the FWHM of the rocking curves were 23.0 and 26.6 arcseconds respectively. Raman spectra were also collected on both types of epi and did not show any differences. This data leads us to conclude that the shift to the HGR process did not adversely affect the epitaxial morphology and quality.

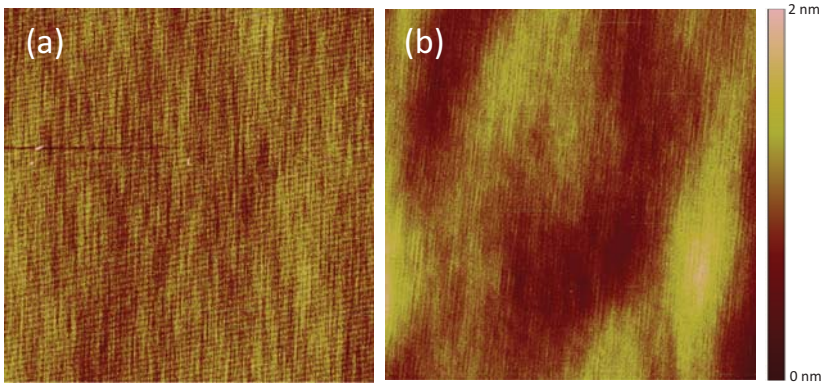

Figure 5. 10µm x 10µm AFM scans of (a) LGR epi (RMS=0.32nm) and (b) HGR epi (RMS=0.34nm)

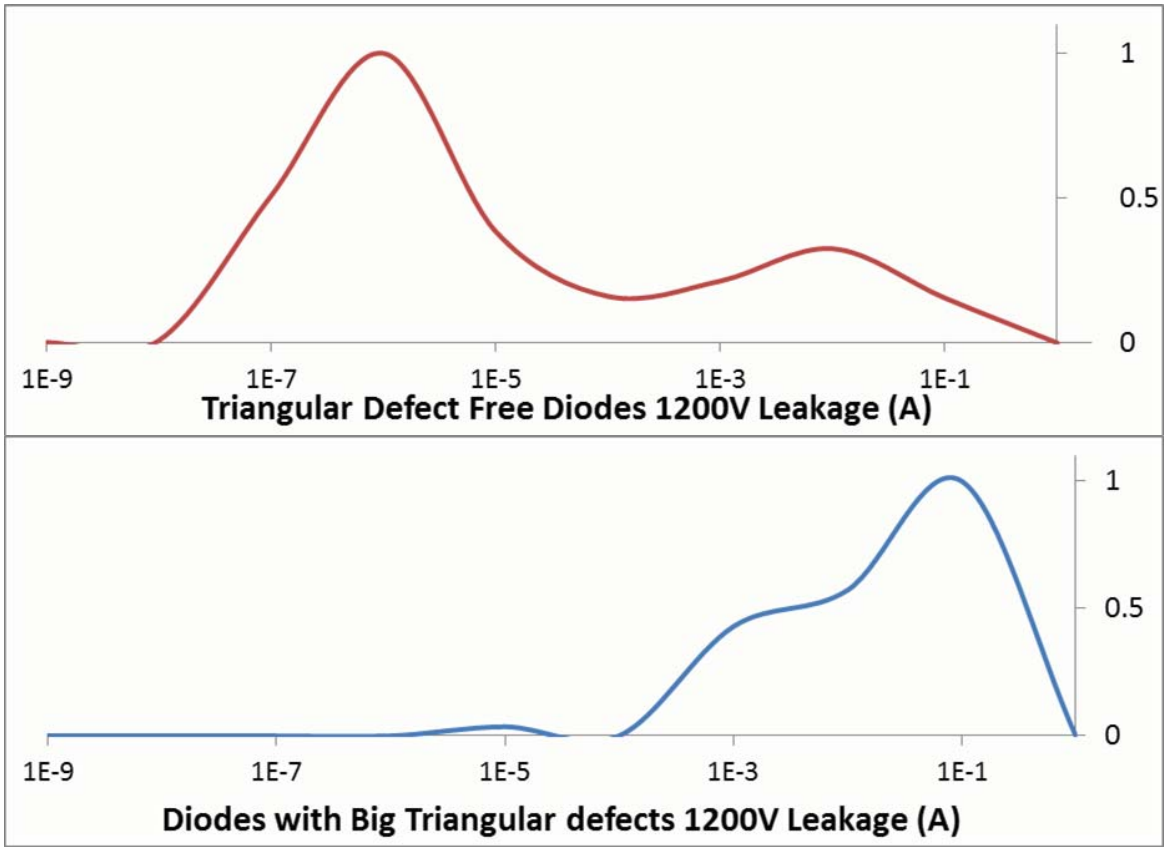

Figure 6. 1200V reverse bias leakage current distributions of diodes with and without large triangular defects

A dense grid of Junction Barrier Schottky (JBS) diodes were fabricated on wafers that had Candela defect maps. The diodes were tested and the results split by the presence or absence of large triangular defects in the Candela scans. Leakage current at 1200V from over 2300 such devices was measured. Figure 6 shows the normalized leakage current frequency distribution of devices with and without big triangular defects in the active diode area. The majority of the diode population without big triangular defects is at 1μA. There is also a small population with a leakage current of 10mA, that are due to the other types of defects as seen under Nomarski and Candela scans. The diodes with the big triangular defects are much leakier with the leakage distribution ranging from 1mA to 100mA. Better classification of the size and type of defects can lead to better understanding of the various leakage populations.

CONCLUSIONS

Large obtuse angled triangular defects were observed in epitaxial layers grown on 100mm 4H-SiC substrates. A combination of higher growth rate and higher Cl/Si ratio was found to drastically reduce the nucleation of these defects. The few triangular defects that formed with the new HGR process were much smaller in size. Molten KOH etching revealed that the larger triangular defects in the LGR epi had a similar core structure as the smaller triangular defects seen in the HGR epi. AFM, XRD and Raman spectra showed no differences in the epitaxial layers grown by the LGR and HGR processes. JBS diodes were fabricated on wafers with large triangular defects. The devices which contained the large triangular defects had much higher leakage currents compared to defect free devices.

REFERENCES

1. T. Ueda, H. Nishino, and H. Matsunami, J. Crys. Growth, Vol. 104, pp. 695 (1990)

2. T. Kimoto, and H. Matsunami, J. Appl. Phys., Vol. 75, pp. 850 (1994)

3. J.A Powell, J.B. Petit, J.H. Edgar, I.G. Jenkins, L.G. Matus, J.W. Yang, P. Pirouz, W.J. Choyke, L. Clemen, and M. Yoganathan, Appl. Phys. Lett., Vol. 59, pp. 333 (1991)

4. A.O. Konstantinov, C. Hallin, O. Kordina, and E. Janzén, J. Appl. Phys., Vol. 80, pp. 5704 (1996)

5. H. Das, G. Melnychuk and Y. Koshka, J. Crys. Growth, Vol. 312, pp. 1912-1919, 2010

6. A. Shrivastava, P. Muzykov, J.D. Caldwell, and T.S. Sudarshan, J. Crys. Growth, Vol. 310, pp. 4443–4450 (2008)

7. G. Chung, M.J. Loboda, J. Zhang, J.W. Wan, E.P. Carlson, T.J. Toth, R.E. Stahlbush, M. Skowronski, R. Berechman, S.G. Sundaresan, and Ranbir Singh, Mater. Sci. Forum Vols. 679-680, pp. 123-126 (2011)

8. H. Das, S. Sunkari, T. Oldham, J. Casady, and Jeff Casady, presented at the 2011 ICSCRM, Invited Poster-3, Cleveland, OH, 2011 (to be published in Mater. Sci. Forum)